

## Tensile strength equation for HSS bracing members having slotted end connections

Sang-Whan Han<sup>1,\*</sup>, Wook Tae Kim<sup>2,§</sup> and Douglas A. Foutch<sup>3,¶</sup>

<sup>1</sup>*Department of Architectural Engineering, Hanyang University, Seoul 133-791, Korea*

<sup>2</sup>*Samsung Engineering and Construction Company, Korea*

<sup>3</sup>*Department of Civil and Environmental Engineering, University of Illinois at Urbana and Champaign, Urbana 61801, U.S.A.*

### SUMMARY

In the previous study, the authors investigated the effect of  $w/t$  ratios on the behaviour of bracing members under symmetric cyclic loading in compression and tension. In this study, 11 bracing members with slotted end sections made of cold-formed square hollow structural sections (HSS) were tested. The  $w/t$  ratios ranged from 8 to 28. Unlike the test results of other former studies obtained under compression-oriented cyclic loading, the results of this study showed that bracing members having a smaller  $w/t$  ratio ( $<14$ ) had less deformation and less energy dissipation capacity, and a shorter fracture life compared with other specimens. Such inferior behaviour resulted from early fracture at the slotted end section. This study compares tensile strength obtained from the design equations in the AISC LRFD manual and Eurocode 3 using the actual strengths of the tested specimens. This study found that for preventing early fracture in HSS bracing members, design fracture strength should be larger than design yield strength. Design strength equations are proposed for bracing members in special concentrically braced frames (SCBF). The proposed design equations are verified by experimental tests conducted under symmetric cyclic loading in tension and compression using two HSS bracing members designed according to the proposed equation. Copyright © 2007 John Wiley & Sons, Ltd.

Received 8 July 2006; Revised 20 November 2006; Accepted 20 November 2006

KEY WORDS: design equation; deformation capacity; fracture life; width–thickness ratio; hollow structural section

\*Correspondence to: Sang-Whan Han, Department of Architectural Engineering, Hanyang University, Seoul 133-791, Korea.

†E-mail: swhan82@hotmail.com

‡Associate Professor.

§Researcher.

¶Professor.

Contract/grant sponsor: SRC/ERC; contract/grant number: R11-2005-056-04002-0

Contract/grant sponsor: Korean Research Foundation; contract/grant number: KRF-2004-013-D00047

## INTRODUCTION

There are two types of braced frames in the current seismic design provisions [1]: concentrically braced frames (CBF) and eccentrically braced frames (EBF). CBF is classified as ordinary CBF (OCBF) or special CBF (SCBF) depending on the design and detail requirements. More stringent design and detail requirements are specified for SCBF, resulting in better seismic behaviour.

The seismic behaviour of bracing members has been investigated by many researchers [2–7]. In particular, several researches [3, 8, 9] evaluated the effect of the width–thickness ratio ( $w/t$  ratio) on the seismic behaviour of bracing members. They observed that under compression-oriented cyclic loading, specimens having a small  $w/t$  ratio had larger deformation capacity than specimens having a large  $w/t$  ratio due to less severe local buckling occurring in the specimens having a small  $w/t$  ratio.

Liu and Goel [9] reported that local buckling at the plastic hinge location in tubular bracing members significantly influences the fracture life of bracing members. According to a study by Uang and Bertero [10], tubular braces are susceptible to failure induced by local buckling and subsequent material fracture. Preventing local buckling in tubular braces is the key to precluding premature material fracture [9]. Uang and Bertero [10] and Tang and Goel [11] proposed width–thickness ratios of  $500/\sqrt{F_y}$  and  $250/\sqrt{F_y}$  for rectangular hollow structural sections (HSS). In the AISC seismic provisions [12], the limiting width–thickness ratio is specified as  $263/\sqrt{F_y}$ , where  $F_y$  (MPa) is the specified minimum yield strength.

Han *et al.* [13] conducted a nonlinear response history analysis of a three-storey SCBF that was designed according to the AISC LRFD manual [14] under severe earthquake ground motions. According to the analysis results, bracing members in the SCBF experienced almost symmetric axial deformation in compression and tension under severe ground motions rather than compression-oriented deformation. Thus, they tested bracing members having slotted end sections under quasi-static cyclic loading which is symmetric in compression and tension instead of compression-oriented cyclic loading. Eleven specimens having square HSS were tested having  $w/t$  ratios ranging from 8 to 28. The details at the connection between the gusset plates and bracing member followed the requirements specified in the AISC HSS connection manual [15] and AISC steel construction manual [14, 16, 17]. The test results showed that specimens having smaller  $w/t$  ratios experienced less severe local buckling and fractured at the mid-section in the later loading cycles.

However, this phenomenon did not hold for specimens having  $w/t$  ratios less than 14. For these specimens, earlier fracture was observed in the specimen with decreasing  $w/t$  ratios. No severe local buckling was detected in these specimens, which resulted in no sectional reduction at the mid-section. In specimens with  $w/t$  ratios of 8 and 11 (S 90-8 and S 69-11), strain concentrated at the slotted end connection under tension led to early fracture in the slotted end section. Due to the early fracture, these two specimens had less deformation and energy dissipation capacity. Specimen (S 90-8) with a  $w/t$  ratio of 8, which was the smallest  $w/t$  ratio (8) among the specimens, had the least deformation capacity and the shortest fracture life among the specimens. Figure 1 shows the measured hysteretic behaviour of specimens having  $w/t$  ratios of 14, 11, and 8 (S 85-14, S 69-11, and S 90-8). It is noted that  $w/t$  ratios of these specimens satisfied the  $w/t$  ratio limit of 18 for SCBF specified in the AISC seismic provisions [12].

The purpose of this study is to investigate the design tensile strength equations specified in the AISC LRFD manual [14] and Eurocode 3 [18] for bracing members in SCBF. This study



DESIGN EQUATION FOR BRACING MEMBERS IN AISC LRFD MANUAL

Bracing members and gusset plates should be designed for tension and compression. The connections and gusset plates should be able to resist the largest forces transferred by the bracing members. Bracing members and gusset plates are connected using weldments and bolts which should resist shear forces transferred by the bracing members. Bracing members should have sufficient strength to resist tension and compression induced by external loads. Design tensile and compressive strength can be calculated by design equations (D1) and (E2) in the AISC LRFD manual [14]. Since the design tensile strength equations strongly relate to member fracture, only design tensile strength equations are summarized and discussed hereafter.

In the AISC LRFD manual [14], the design tensile strength ( $\phi P_n$ ) is the smaller of two values calculated from the two equations shown in Equation (1) in which  $0.75A_e F_u$  and  $0.9A_g F_y$  are the design strength equation for effective net section fracture and gross section yielding, respectively

$$\phi P_n = \min(0.75A_e F_u, 0.9A_g F_y) \tag{1}$$

where  $A_e$  is the effective net area,  $A_g$  is the gross area,  $F_u$  is the specified minimum tensile strength, and  $F_y$  is the specified minimum yield strength. Figure 2 shows the connection details of HSS bracing members specified in the AISC LRFD manual [14], AISC HSS connection manual [15], and AISC steel construction manual [16]. As shown in Figure 2, HSS bracing members have

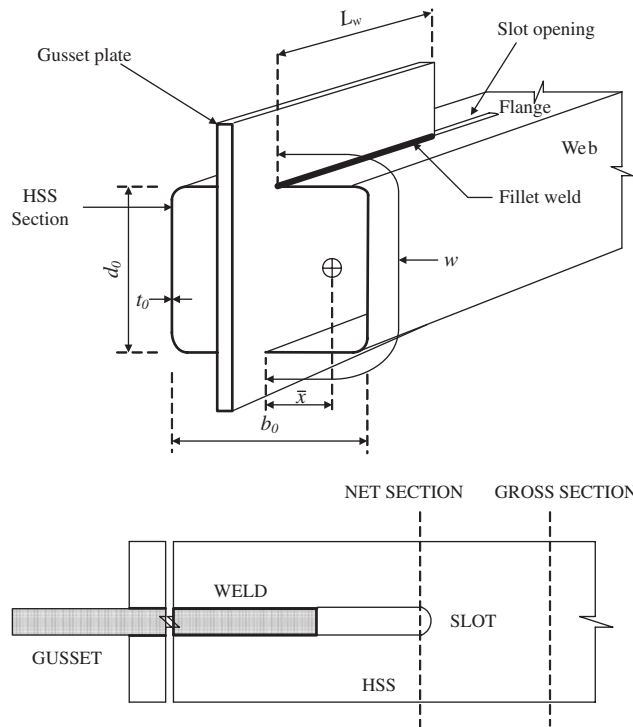


Figure 2. Details of slotted end connections in HSS bracing members.

slotted holes for connecting to the gusset plates, thereby the net area passing through the slotted sections is smaller than the gross area ( $A_g$ ) of the HSS sections. In Equation (1), the effective net area ( $A_e$ ) is calculated using the following equations:

$$A_e = A_n U \quad (2)$$

$$A_n = A_g - 2t \times t_0 \quad (3)$$

$$U = 1 - (\bar{x}/L_w) \leq 0.9 \quad (4)$$

$$\bar{x} = \frac{b_0^2 + 2b_0d_0}{4(b_0 + d_0)}$$

where  $A_n$  is the net area,  $t_0$  is the thickness of HSS, and  $t$  is the gusset plate thickness,  $L_w$  is the weld length,  $d_0$  is the sectional width and  $b_0$  is the depth.

### NEW DESIGN TENSILE STRENGTH EQUATION

As mentioned earlier, the design tensile strength of bracing members in the AISC LRFD manual [14] is defined as the smaller value between the design yield strength of the gross section ( $0.9A_gF_y$ ) and design fracture strength of the net section ( $0.75A_eF_u$ ). In the previous study conducted by Han *et al.* [13], the design tensile strength ( $\phi P_n$ ) of the specimens having slotted end sections was the design fracture strength ( $0.75A_eF_u$ ), because it was smaller than the design yield strength ( $0.9A_gF_y$ ).

Even though specimens were designed in compliance with Equation (1), previous study [13] observed that specimens having small  $w/t$  ratios experienced early fracture at the slotted end section. In contrast, specimens having larger  $w/t$  ratios experienced severe local buckling at the mid-section as shown in Figure 4 before yielding occurred in the slotted end sections. The specimens fractured at the mid-section during tensile loading cycles before the slotted end sections fractured. Severe local buckling resulted in significant reduction of the sectional area at the mid-section. It is noted that the specimens having larger  $w/t$  ratios also did not pass Equation (3).

To prevent early fracture at the slotted end sections, particularly in specimens having small  $w/t$  ratios, the design equation in Equation (1) should be modified so that the design fracture strength of the net section ( $0.75A_eF_u$ ) is larger than the design yield strength of the gross section ( $0.9A_gF_y$ ), as follows:

$$0.75A_eF_u > 0.9A_gF_y \quad (5)$$

By rearranging Equation (5), the following equation can be obtained:

$$A_e/A_g > 1.2F_y/F_u \quad (6)$$

Application of the above equations to the bracing members could lead to yield before fracture at the slotted end sections. In the Eurocode 3, the following equation is proposed for ductile behaviour of tension members:

$$0.9[A_{net}/A] \geq [f_y/f_u][\gamma_{M2}/\gamma_{M0}] \quad (7)$$

Table I. Results of coupon tests.

Specimen	Young's modulus ( $E$ , MPa)	Yield strength ( $F_y^{(*)}$ , MPa)	Ultimate strength ( $F_u^{(*)}$ , MPa)	Yield ratio ( $F_y^{(*)}/F_u^{(*)}$ )	Elongation strain (%)
S 90-8	197 310	425	456	0.93	31.1
S 69-11	198 470	402	462	0.87	29.8
R 90-8	189 563	387	438	0.88	28.7
R 69-11	193 110	394	448	0.88	28.9

S(R) 90-9

(1) Effective slenderness ratio

(1) (2)

(2) Width–thickness ratio

S, HSS specimen; R, HSS specimen reinforced at the slotted end sections

Note that minimum specified yield and ultimate strength ( $F_y$ ,  $F_u$ ) of SPSR 400 are 317 and 400 MPa, respectively, ( $F_y/F_u = 0.79$ ).  $F_y^{(*)}$ ,  $F_u^{(*)}$  are the actual yield and ultimate strength obtained from coupon tests.

where  $A = A_g$ ,  $A_{net} = A_e$ ,  $f_y = F_y$ ,  $f_u = F_u$ ,  $\gamma_{M2} = 1.25$ , and  $\gamma_{M0} = 1.1$ . By rearranging Equation (7), the following equation can be obtained:

$$A_e/A_g \geq 1.26 F_y/F_u \quad (8)$$

#### APPLICATION OF THE PROPOSED EQUATION

The above equations were applied to the 11 specimens with  $w/t$  ratios ranging from 8 to 28 tested in the previous study [13]. All specimens do not satisfy Equation (6). Two specimens (S 90-8 and S 69-11) with the smallest  $w/t$  ratios of 8 and 11 experienced early fracture at the slotted end sections, whereas in the other specimens fractured at the mid-sections due to the severe local buckling at the mid-section. Table I shows the results of coupon tests. Table II shows application results of Equations (6) and (8). According to this table, Equations (6) and (8) accurately predicted early fracture at the net sections ( $A_e/A_g < 1.2 F_y/F_u$ ,  $A_e/A_g < 1.26 F_y/F_u$ ) in specimens having small  $w/t$  ratios. To prevent early fracture in these specimens, Equation (6) or (8) should be satisfied.

#### EXPERIMENTAL TEST FOR VERIFICATION OF THE PROPOSED EQUATION

In this study, two test specimens, R 90-8 and R 69-11, were made which had the same configurations and dimensions as specimen S 90-8 and S 69-11 ( $w/t$  ratio = 8 and 11) except for the sectional area in the slotted ends. In specimen R 90-8 and R 69-11, the slotted ends were reinforced to satisfy Equation (6) as shown in Table II and Figure 3. The dimensions of reinforcing steel plates are given in Figure 3, which were attached to the slotted end sections using filled welds along the four corners of the plate. A slotted hole was cut from the plates for installation. The material properties of plates were the same as those of the specimens.

Figure 4 shows the details of the specimens. The test was carried out under symmetric cyclic loading in compression and tension. A previous study [13] shows that symmetric displacement loading is more appropriate for the test of bracing members in SCBF. The loading protocol

Table II. Properties of specimens.

Specimen	Section (width × thickness) (mm)	$A_g^{(1)}$ (cm <sup>2</sup> )	$A_{net}^{(2)}$ (cm <sup>2</sup> )	$L_w^{(3)}$ (cm)	$\bar{X}^{(4)}$ (cm)	$\bar{X}/L_w^{(5)}$	$U^{(6)}$	$A_e^{(7)}$ (cm <sup>2</sup> )	$A_e/A_g^{(8)}$	$1.2F_y/F_u^{(9)}$ (proposed)	$1.26F_y/F_u^{(10)}$ (Eurocode 3)	$\frac{(8)}{(9)}$	$\frac{(8)}{(10)}$	Fracture location
S 90-8	100 × 100 × 9	30.7	27.3	25.1	3.75	0.15	0.85	23.20	0.76			0.8	0.76	S <sup>+</sup>
R 90-8	100 × 100 × 9	30.7	42.9	25.1	3.75	0.15	0.85	36.50	1.19	0.95	1.0	1.25	1.19	M <sup>++</sup>
S 69-11	125 × 125 × 6	39.67	35.7	22.9	4.69	0.20	0.80	28.41	0.72			0.75	0.72	S
R 69-11	125 × 125 × 6	39.67	49.4	22.9	4.69	0.20	0.80	43.14	1.09			1.15	1.10	M

Note: <sup>(1)</sup> Gross area of HSS, <sup>(2)</sup> net area of HSS, <sup>(3)</sup> length of the weld to HSS, <sup>(4)</sup> width of HSS section, <sup>(5)</sup> depth of HSS section, <sup>(6)</sup> reduction factor of shear lag effect, <sup>(7)</sup> effective area of HSS, <sup>(8)</sup> ratio of (9) to (1), <sup>(9)</sup> design yield ratio of SPSR 400, <sup>(10)</sup>  $F_y$  is the specified minimum yield strength, <sup>(11)</sup> the specified minimum tensile strength, S<sup>+</sup> the fracture at the slotted end section, and M<sup>++</sup> the fracture at the mid-section.

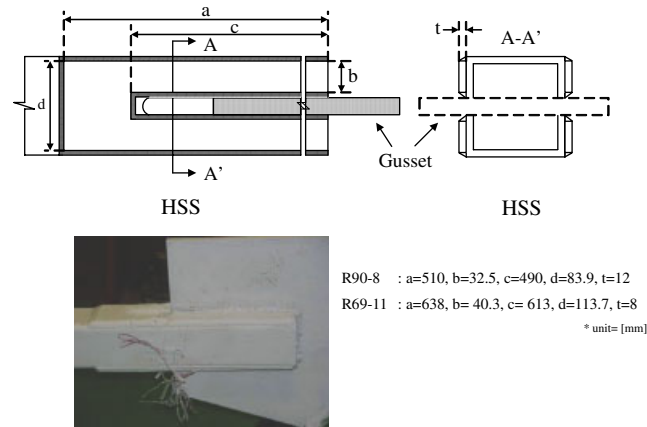


Figure 3. Reinforcement at the slotted end connection.

prescribed in SAC (1997) was adopted with a small modification in the first few cycles to detect the buckling point. Thus, up to the buckling load calculated using Equation (E2-2,3) in the AISC LRFD manual (2001), the loading cycle was controlled by force. After the buckling force was detected, the loading cycle was controlled by displacement. Loading was applied until the specimen fractured.

Figure 5 shows the test set-up and loading cycle. A loading frame with a hinge at each corner was made. Hinge conditions were achieved by installing bearings at the four corners of the frame. Specimens were installed diagonally in the loading frame. To prevent instability of the loading frame, lateral bracing was installed.

According to the test results of specimen R 90-8 ( $w/t$  ratio = 8), local buckling occurred and the specimen failed in the mid-section of the member. It is noted that specimen S 90-8 fractured at the slotted end section and did not experience local buckling. Figure 6 shows the final failure mode for specimens S 90-8 and R 90-8. The failure sequences between specimens S 90-8 and R 90-8 and specimens S 69-11 and R 69-11 are different. As shown in Figure 6, both specimens (S 90-8 and S 69-11) first experienced overall buckling (i), followed by significant elongation of slotted end section (ii) and then fractured (iv) at the slotted end sections before local buckling occurred at the mid-section (iii). Figure 6(b) shows the sequence of failure for specimens R 90-8 and R 69-11. In these specimens local buckling (ii) was observed at the mid-sections after overall buckling (i). The specimens fractured (iv) at the mid-section before the slotted end sections fractured.

The occurrence of local buckling in R 90-8 and R 69-11 is solely attributed to the strengthening of the slotted end connections according to the proposed design equation. Longer fracture life and greater deformation capacity were observed in specimens R 90-8 and R 69-11 since early fracture at the slotted end sections did not occur in these specimens.

Figure 7 shows the cycle number occurring at which overall buckling, local buckling, and fracture occurred for each specimen. In specimen R 90-8, local buckling occurred in cycle 17 and specimen failed at the mid-section during cycle 20. Specimen S 90-8, however, fractured during cycle 15 at the slotted end soon after overall buckling occurred without any local buckling. Thus, specimen R 90-8 experienced more displacement cycles until fracture. A similar observation was made for specimens S 69-11 and R 69-11 both with  $w/t$  ratios of 11. Specimens S 69-11 and R 69-11 failed during cycles 17 and 20, respectively.

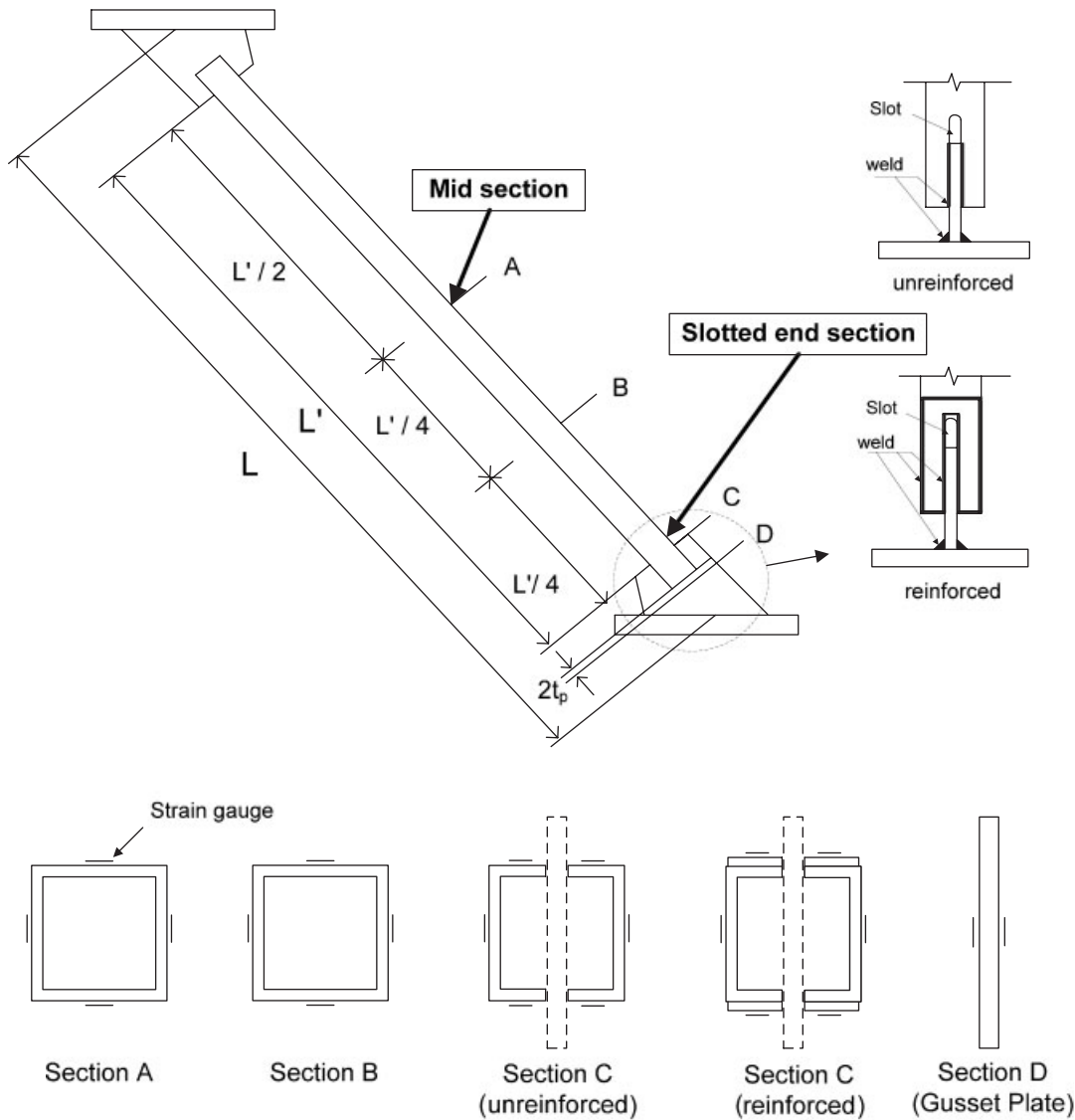


Figure 4. Specimen details.

Figure 7 also shows that the deformation capacities of specimens (S 82-19, S 80-22, S 77-28) not satisfying the  $w/t$  ratio limit ( $= 18$ ) for SCBF decreased as the  $w/t$  ratios were increased due to the significant local buckling, which led to a large reduction of sectional area at the mid-section during early loading stage. Thus, specimens having large  $w/t$  ratios also experience early fracture at the mid-section instead of at the slotted end sections. Figures 8(a) and (b) plot for the envelope curves extracted from the hysteretic curves of specimen S 90-8 and R 90-8, and S 69-11 and

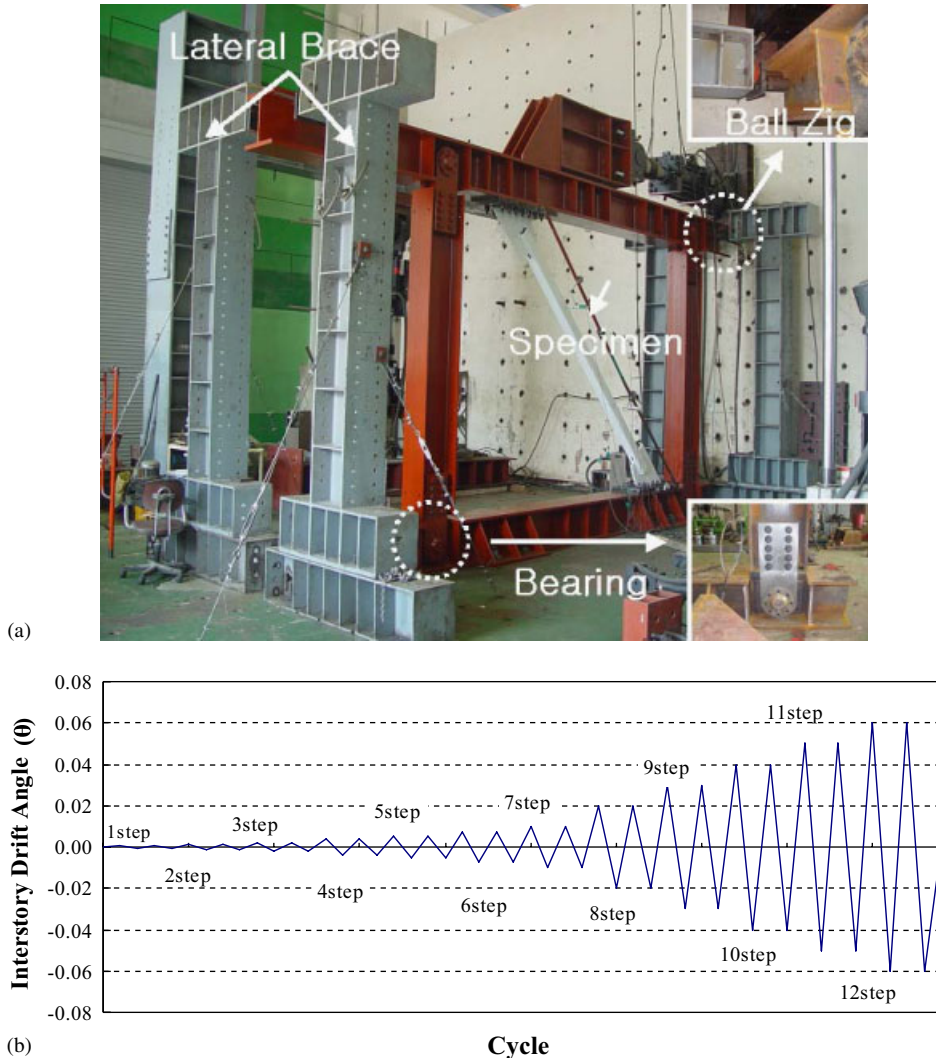


Figure 5. (a) Test set-up; and (b) loading cycles.

R 69-11. Figures 8(a) and (b) show that specimens R 90-8 and R 69-11 have fuller hysteretic curves than corresponding specimens S 90-8 and S 69-11.

Figure 9 shows the energy dissipation capacity normalized by tensile yield load ( $P_y$ )  $\times$  yield displacement ( $\Delta_y$ ) until fracture. Energy dissipation capacity is calculated by summing the area under the hysteretic curve from the initial loading stage to fracture. Yield load ( $P_y$ ) and yield displacement ( $\Delta_y$ ) are determined from bilinear representation of the envelope of actual hysteretic curves. Normalization is meaningful since this process eliminates the effects resulting from variations in material property, cross-sectional area, and specimen length [4]. According to Figure 9 specimens R 90-8 and R 69-11 have 1.4 and 4 times the energy dissipation capacity of the



Figure 6. Buckling and fracture of specimens: (a) S 90-8 and S 69-11; and (b) R 90-8 and R 69-11.

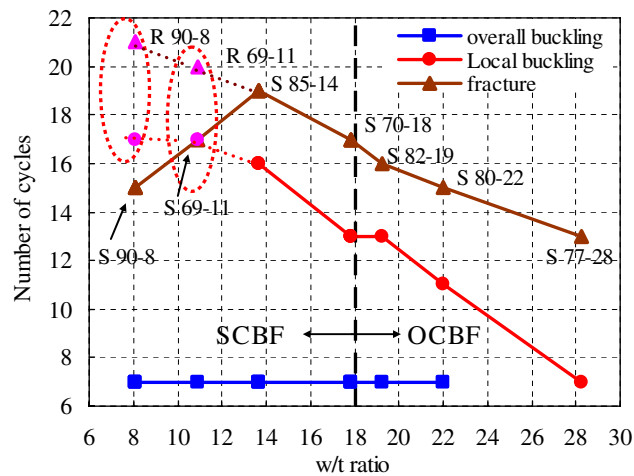


Figure 7. Buckling cycles and fracture cycles of specimen R 90-8 and R 90-12. Note that S(R) 90-9: S, HSS specimen; R, HSS specimen reinforced at the slotted end sections. (1) Effective slenderness ratio and (2) Width–thickness ratio.

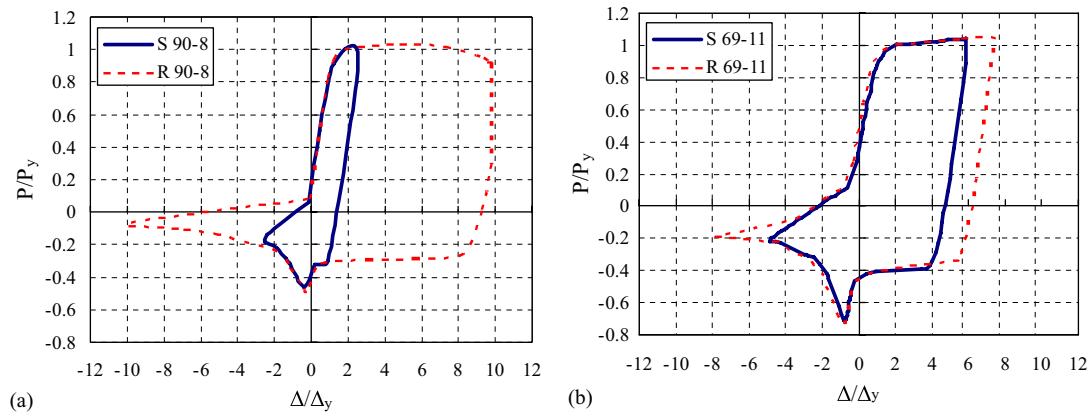


Figure 8. Envelope curves of the specimens: (a) S 90-8 and R 90-8; and (b) S 69-11 and R 69-11.

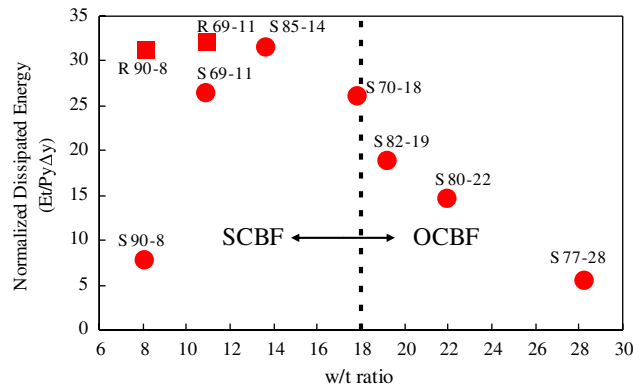


Figure 9. Normalized dissipated energy of specimens. Note that S(R) 90-9: S, HSS specimen; R, HSS specimen reinforced at the slotted end sections. (1) Effective slenderness ratio and (2) Width–thickness ratio.

corresponding specimens S 90-8 and S 69-11, respectively. Thus, HSS bracing members having slotted end connections with small  $w/t$  ratios ( $<14$ ) designed according to Equations (1) and (3) have longer fracture life, larger deformation and energy dissipation capacity. It is also noted that energy dissipation capacity of specimens (S 82-19, S 80-22, S 77-28) not satisfying the  $w/t$  ratio limit for SCBF becomes smaller with increasing  $w/t$  ratios.

## CONCLUSIONS AND RECOMMENDATIONS

This study proposed a design tensile strength equation for cold-formed HSS bracing members with slotted end connections in order to improve the deformation and energy dissipation capacity. The

major findings and conclusions are summarized as follows:

- (1) Early fracture was observed at the slotted end sections in specimens for HSS bracing members having small  $w/t$  ratios designed according to AISC LRFD manual. It is worthy to note that in AISC-LRFD manual, such members are classified ductile bracing members in SCBF.
- (2) The proposed design tensile strength equation for cold-formed HSS bracing members with slotted end sections used in SCBF is as follows:

$$A_c/A_g > 1.2y F_y/F_u$$

- (3) The design equations specified in Eurocode 3 [18] also accurately predict early fracture at the slotted end sections of HSS bracing members. Thus, this equation can be also used for designing ductile HSS bracing members in SCBF.
- (4) Test results show that cold-formed HSS bracing members that satisfy the proposed equation have longer fracture life, and larger deformation and energy dissipation capacity.

#### ACKNOWLEDGEMENTS

The work presented in this paper was sponsored by SRC/ERC R11-2005-056-04002-0 and Korean Research Foundation (KRF-2004-013-D00047). The views expressed are those of authors, and do not necessarily represent those of the sponsor. The comments by two anonymous reviewers are greatly acknowledged.

#### REFERENCES

1. International Code Council. *International Building Code*. January 2003.
2. Khan LF, Hanson RD. Inelastic cycles of axially load steel members. *Journal of the Structural Division (ASCE)* 1996; **102**(90):947–959.
3. Jain AK, Goel SC, Hanson RD. Hysteretic response of restrained steel tubes. *Journal of Structural Engineering (ASCE)* 1978; **104**(6):897–910.
4. Popov EP, Black RG. Steel struct under severe cyclic loadings. *Journal of the Structural Division (ASCE)* 1981; **107**(9):1857–1881.
5. Marino EM, Nakashima M. Seismic performance and new design procedure for chevron braced frames. *Earthquake Engineering and Structural Dynamics* 2006; **35**:433–452.
6. Shibata M *et al*. Elastic–plastic behavior of steel braces under repeated cyclic loading. *Proceedings of the 5th World Conference on Earthquake Engineering*, Rome, 1973; 845–848.
7. Tremblay R. Inelastic seismic response of steel bracing members. *Journal of Constructional Steel Research* 2002; **58**:665–671.
8. Lee SS, Goel SC. Seismic behavior of hollow and concrete-filled square tubular bracing members. *Report No. UMCE 87-11*, Department of Civil Engineering, The University of Michigan, Ann Arbor, 1987.
9. Liu Z, Goel SC. Investigation of concrete filled steel tubes under cyclic bending and buckling. *Report No. UMCE 87-3*, The University of Michigan, Ann Arbor, 1987.
10. Uang CM, Bertero VV. Earthquake simulation tests and associated studies of a 0.3-scale model of a six storey centrally braced steel structure. *Report No. UCB/EERC-86/10*, Earthquake Engineering Research Center, University of California, Berkeley, 1986.
11. Tang X, Goel SC. Seismic analysis and design consideration braced steel structures. *Report No. UMCE 87-4*, The University of Michigan, Ann Arbor, 1987.
12. AISC. *Seismic Provision for Structural Steel Buildings*. AISC: Chicago, IL, 2002.
13. Han SW, Kim WT, Foutch D. Experimental study of HSS braces under cyclic loads. *SRS No. 641*, Department of Civil and Environmental Engineering, University of Illinois at Urbana-Champaign, Urbana, IL, June 2006.

14. AISC. *Manual of Steel Construction* (LRFD 3rd edn). AISC: Chicago, IL, 2001.
15. AISC. *Hollow Structural Sections Connections Manual*. American Institute of Steel Construction: Illinois, 1997.
16. AISC. *Steel Construction Manual*, vol. I and II. AISC: Chicago, IL, 2005; 16.1-251.
17. Tamboli AR. *Handbook of Structural Steel Connection Design and Details*. McGraw-Hill: New York, 1999.
18. The European Committee for Standardization. *Eurocode 3: Design of Steel Structures*. DD ENV 1993-1-1, ENV, 1992.